



Contents lists available at ScienceDirect

Journal of Quantitative Spectroscopy & Radiative Transfer

journal homepage: www.elsevier.com/locate/jqsrt

Non-Voigt line-shape effects on retrievals of atmospheric ozone: Collisionally isolated lines

H. Tran^a, F. Rohart^b, C. Boone^c, M. Eremenko^a, F. Hase^d, P. Bernath^e, J.-M. Hartmann^{a,*}^a Laboratoire Interuniversitaire des Systèmes Atmosphériques (LISA), CNRS/INSU (UMR 7583), Universités Paris XII et Paris VII, Université Paris XII, 94010 Créteil Cedex, France^b Laboratoire de Physique des Lasers, Atomes et Molécules (PhLAM), UMR CNRS 8523, Centre d'Etudes et Recherches Lasers et Applications, Université de Lille 1, 59655 Villeneuve d'Ascq Cedex, France^c Department of Chemistry, University of Waterloo, Waterloo, Ontario, Canada N2L 3G1^d KIT, Institute of Meteorology and Climate research (IMK) PO Box 3640, D-76021 Karlsruhe, Germany^e Department of Chemistry, University of York, Heslington, York, UK YO10 5DD

ARTICLE INFO

Article history:

Received 11 February 2010

Accepted 6 April 2010

Keywords:

Ozone

Speed dependence

Atmospheric retrievals

ABSTRACT

This paper addresses the question of errors in retrievals of vertical profiles of ozone from atmospheric spectra caused by assuming that the absorption lines have pure Voigt line shapes. The case of collisionally isolated transitions (no line mixing) is treated by considering only the effects of the speed dependence (SD) of the pressure broadening. The case of O₃ retrievals from a sequence of limb transmission spectra is first treated theoretically. The results show that the influence of SD is very small, leading to changes in the residuals and in the retrieved O₃ mixing ratios smaller than 1%. These findings are then confirmed by treating a series of spectra recorded by the ACE-FTS instrument. Similar exercises are also made for other observation techniques by treating simulated or measured limb and nadir emission spectra as well as ground-based solar and in-situ laser transmission data. All lead to the general conclusion that SD (and Dicke narrowing) can be neglected in retrievals of ozone amounts from recorded atmospheric spectra. Indeed, the biases caused in the ozone profiles by the use of pure Voigt line shapes still remain significantly smaller than the total error/uncertainty from other sources such as improper line intensities and widths, uncertainty in the instrument function, errors in the pressure and temperature profiles and so forth.

© 2010 Elsevier Ltd. All rights reserved.

1. Introduction

Deviations of absorption lines from the Voigt profile have been the subject of many experimental and theoretical studies. They result from collision-induced changes of the velocity of the optically active molecule and from the speed dependence of the pressure-broadening and pressure-shifting coefficients of the transitions. An extensive review of these phenomena has been given in Chapt. III of Ref. [1] for the core region of collisionally isolated lines (i.e., in the absence of line-mixing effects

discussed in Chapt. IV of Ref. [1]). With a collision partner such as N₂ (and air), and except for molecules with large rotational constants (H₂, HCl, H₂O, CH₄), the spectral consequences of these “velocity effects” are generally of the order of one percent. This is likely why there have been very few studies [2–6] of the influence of these processes on atmospheric spectra and of their effect on remote sensing retrievals. To our knowledge, these questions remain open in the particular case of ozone, in spite of the considerable importance of precise monitoring of this molecule in our atmosphere. The present paper provides a quantitative analysis for O₃ sounding from infrared absorption and emission spectra recorded with various techniques including limb, nadir, ground-based and in situ observations.

* Corresponding author. Tel.: +33 145176542; fax: +33 145171558.
E-mail address: hartmann@lisa.univ-paris12.fr (J.-M. Hartmann).

For ozone lines, Rohart and co-workers [7,8] have provided significant information on the deviations from the Voigt profile due to velocity effects. They found the expected small (typically less than 2%) deviations from the Voigt profile using high signal-to-noise ratio laboratory measurements. They also showed that for systems like O_3/N_2 and O_3/O_2 accurate line-profile descriptions can be obtained by accounting only for the speed dependence of the collisional broadening and disregarding the influence of velocity changes (Dicke narrowing) (see also Refs [9,10] and those therein). Starting from the results of Ref. [8], we have built a simple but realistic speed-dependent Voigt (SDV) model applicable to all O_3 transitions. It is first used for theoretical simulations using standard atmospheric profiles and radiative transfer calculations for a series of atmospheric limb-transmission spectra in the $10\ \mu\text{m}$ region (v_1 and v_3 bands) for various lines of sight (i.e., tangent heights). These correspond to situations representative of satellite-borne limb-viewing solar absorption experiments such as the Atmospheric Chemistry Experiment-Fourier Transform Spectrometer (ACE-FTS) [11]. The resulting tangent-altitude dependent spectra have then been fitted using an inversion procedure in which Voigt line shapes are used in order to retrieve the O_3 vertical profile. The results of this theoretical test carried out with two different retrieval codes in France and Canada show that the errors in the retrieved O_3 profile and in observed minus calculated spectral residuals are always smaller than 1%. This upper limit is then confirmed with a sequence of measured transmission spectra recorded by the ACE-FTS [11] instrument. Similar exercises are also made with emitted radiances in limb-viewing and nadir observations as well as absorptions in ground-based solar and in situ spectra. This extends the study to situations representative of, for instance, the Michelson Interferometer for Passive Atmospheric Sounding [12] (MIPAS, limb emission), the Infrared Atmospheric Sounding Interferometer [13] (IASI) and the Atmospheric InfraRed Sounder [14] (AIRS), ground-based spectrometers such as those of the Network for the Detection of Atmospheric Composition Change (NDACC, <http://www.ndacc.org/>), and the in-situ laser absorption instrument SPectroscopic Infra Rouge par Absorption de Laser Embarqués [15] (SPIRALE).

The conclusion of all these exercises is that the consequences of speed dependence (and of Dicke narrowing) can be neglected in ozone atmospheric retrievals at this time. Indeed, the errors in the residuals and ozone amounts caused by their neglect remain significantly smaller than those arising from other sources (largely the spectroscopic parameters, but also the atmospheric state and instrument function). This validates the use of Voigt line shapes for isolated lines (no line mixing: a problem that remains to be studied for O_3). This conclusion may have to be reconsidered following future improvements of spectroscopic knowledge and instrumentation.

2. Line-shape model

Following Ref. [8], we only consider the influence of the speed dependence (SD) of the (Lorentz) collisional width Γ on the line shape and thus use a speed-dependent

Voigt (SDV) profile. For its description, we assume that the dependence on the relative speed v_r takes the form $\Gamma(v_r) \propto v_r^\alpha$. This is equivalent to assuming resonant collisions and a dominant single term in the expansion of the intermolecular potential V with respect to the intermolecular distance R [i.e., $V(R) \propto 1/R^q$] since one then has [1,16,17] $\alpha = (q-3)/(q-1)$. This widely used approach is convenient because one can relate the α parameter to the temperature exponent n of the broadening (such that $\Gamma(T) = \Gamma(T_0)(T_0/T)^n$ for which a value is given, for each line, in the HITRAN database [18]). Indeed, neglecting the (small) spacing between the N_2 and O_2 rotational states, one then has: [1] $n = 1 - (\alpha/2) = (q+1)/(2q-2)$. Note that, for the dominant quadrupole–quadrupole interaction involved in O_3 –air collisions, $q=5$, leading to $n=0.75$ which is close to the observed values ($n=0.7$ for dispersive forces with R^{-6}).

For each line, we thus start from the exponent n of the broadening from HITRAN [18] and deduce $\alpha = 2(1-n)$. By averaging $\Gamma(v_r = ||\vec{v}_a - \vec{v}_p||)$ over the Boltzmann distribution of the perturber velocity \vec{v}_p , we then obtain the dependence of the broadening on the absolute speed v_a of the active molecule (O_3). Introducing the average broadening $\Gamma_0 = \langle \Gamma(v_r) \rangle = \langle \Gamma(v_a) \rangle$, and the ratio of the masses of the collision partners $\lambda = m_p/m_a$ ($a=O_3$, $p=N_2$ or O_2) and the most probable O_3 speed $v_a^0 = \sqrt{2k_B T/m_a}$, one has [1,17]

$$\frac{\Gamma(v_a)}{\Gamma_0} = \frac{1}{(1+\lambda)^{\alpha/2}} M\left[-\frac{\alpha}{2}; \frac{3}{2}; -\lambda(v_a/v_a^0)^2\right], \quad (1)$$

where $M(a;b;x)$ is the confluent hypergeometric function [19]. For practical computations of SDV profiles, it is more convenient to use a quadratic law, i.e. [8,20]

$$\Gamma(v_a) = \Gamma_0 + \Gamma_2 \left[(v_a/v_a^0)^2 - \frac{3}{2} \right]. \quad (2)$$

We have thus calculated $\Gamma(v_a)$ from Eq. (1) for various values of n (via α) and have then adjusted the results through Eq. (2). This leads to very good fits and to the empirical function

$$\Gamma_2/\Gamma_0 = 0.27 \times (1-n), \quad (3)$$

relating Γ_2/Γ_0 to n . Note that, for the typical value $n=0.75$, [18] Eq. (3) leads to $\Gamma_2/\Gamma_0 \approx 0.07$ which is consistent with experimentally determined values [7,8].

In summary, starting from the $\Gamma(T_0)$ and n parameters stored in HITRAN we deduce $\Gamma_0 = \Gamma(T) = \Gamma(T_0)(T_0/T)^n$ and $\Gamma_2/\Gamma_0 = 0.27(1-n)$. We then can calculate the SDV profile of each line, including the Doppler effect, by using the Fourier transform of the dipole correlation function [8]. The associated pure Voigt line shapes are obtained with the same procedure by setting $\Gamma_2/\Gamma_0 = 0$. We note again that the differences between the Voigt and SDV profiles are typically less than 2% [7,8].

3. Atmospheric retrievals and discussion

3.1. Limb-viewing sequences

A radiative transfer code was built at LISA in Créteil to simulate atmospheric transmission and emission spectra.

The atmosphere was divided into 1 km layers for altitudes from 0 to 90 km. Profiles of temperature, total pressure and ozone volume mixing ratio (vmr) were taken from the AFGL standard atmospheres [21]. In each layer, the absorption coefficient was calculated over the entire 10 μm ozone band, from 970 to 1070 cm^{-1} with a step of 0.0003 cm^{-1} , using the SDV line shape described in Section 2. Only O_3 lines were taken into account (no solar lines, no absorption by other species). From these data, spectra were calculated, simulating various observation techniques, resolutions and geometries, and then inverted to obtain the ozone vertical distribution using a spectral model that assumes pure Voigt line shapes.

3.1.1. Limb-absorption measurements

Satellite limb-viewing (solar absorption) atmospheric transmission spectra for lines of sight with tangent altitudes from 1 to 90 km with a step of 1 km were first simulated. These transmission spectra were then inverted using a simple (no constraints or regularization) least-squares procedure that minimizes (using the retrieved O_3 vmr profile) the overall rms deviation between the input (SDV) and fitted (Voigt) spectra for all retained wavenumbers and tangent altitudes. This was done using all wavenumbers and a set of micro-windows. In fact, retrievals from high resolution instruments operating in the infrared typically employ micro-windows rather than a more time-consuming analysis of the entire spectrum. Micro-windows are narrow spectral regions containing spectral features from the target molecule, generally with minimal contributions to the spectrum from other

molecules. Therefore, in order to evaluate SDV effects in the context of atmospheric retrievals, O_3 retrievals were also performed on the synthetic spectra employing a set of 36 micro-windows (used in the version 2.2 “ O_3 update” retrievals for the ACE-FTS) spanning a wavenumber range 985–1128 cm^{-1} and an altitude range 5–90 km. The results of various retrievals are displayed in Fig. 1, and examples of the “observed” minus calculated residuals in a micro-window are shown in Fig. 2. Note at this stage that errors in the O_3 vmr and in the transmissions are always less than 1% in magnitude. Also note that the peak in the errors near 40 km in the right panel of Fig. 1 results from the fact that at this altitude there is a switch in the micro-window set that is being used.

The same exercise was carried independently at the Department of Chemistry in Waterloo, using the forward model and its associated inversion scheme described in Ref. [22]. Only the micro-windows currently employed for ACE-FTS spectra were used together with the appropriate instrument function. The results obtained are quantitatively consistent with those obtained at LISA with errors again always less than 1%. Slight differences in the vertical distribution of the error in the O_3 vmr, as compared to the results obtained at LISA, are due to the use of different micro-windows and instrument functions, retrieval schemes, and profiles of pressure, temperature and O_3 vmr.

Finally, Figs. 3 and 4 present the results of a treatment of an occultation sequence of observed spectra measured by the ACE-FTS instrument (occultation ss28648, measured 7 December 2008, latitude 44.94°N, longitude 18.34°W). They confirm the theoretical predictions and

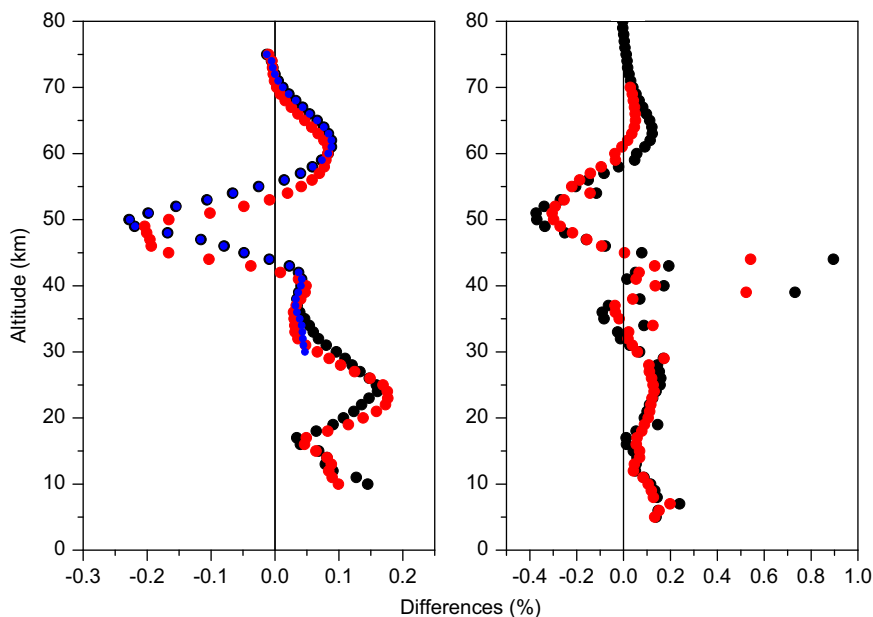


Fig. 1. Relative errors in the O_3 profiles obtained from various fits of simulated atmospheric transmission limb spectra caused by neglecting the speed dependence of the line broadening. Left panel: obtained using high resolution spectra over the entire O_3 band (970–1070 cm^{-1}) in the retrievals starting from 10 km altitude in the case of standard mid-latitude winter (●) and mid-latitude summer (●) profiles. (●) are results obtained with the mid-latitude winter profile in a similar way except that the retrieval only uses spectra with tangent altitudes above 30 km. Right panel: obtained using a set of 36 micro-windows from 985 to 1128 cm^{-1} with spectra at high resolution (●) and those degraded to a resolution of 0.02 cm^{-1} with a Gaussian instrument function (●).

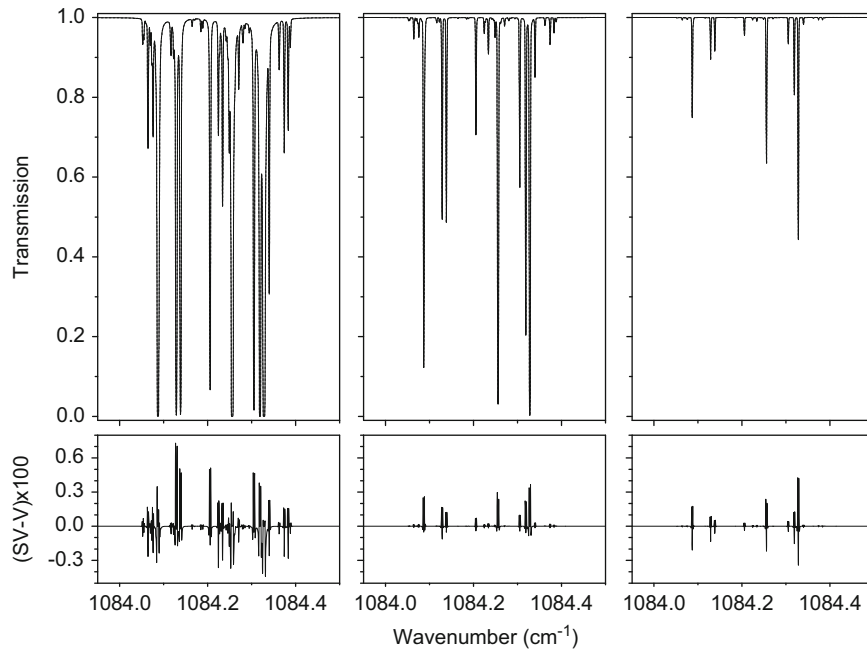


Fig. 2. High resolution O_3 transmission spectra (top) and fit residuals (bottom) due to speed dependence in a micro-window obtained from spectra for three different tangent altitudes, from left to right: 35, 45 and 55 km.

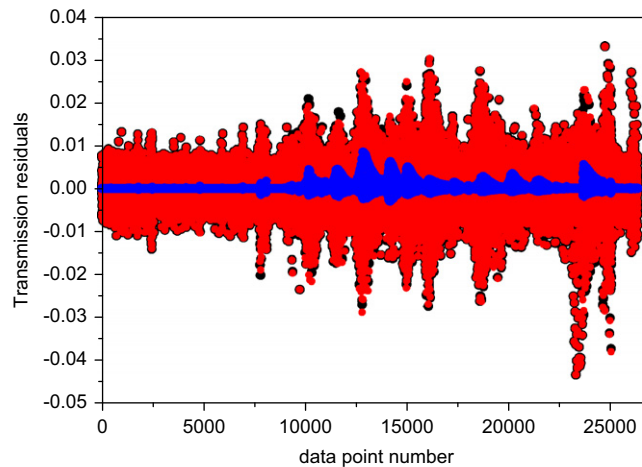


Fig. 3. Residuals obtained in the fit of a real ACE occultation (ss28648) using the ● Voigt model, ● the SDV model. ● are the differences SDV-Voigt. All spectral points of all micro-windows and all tangent heights are included in the data points. From left to right, tangent altitudes vary from about 95 down to 7.5 km.

show that the inclusion of SD in the fits leads to a relatively small change in the residuals (Fig. 3). In fact, most of the fitting errors are from other sources including incorrect line intensities and/or broadening coefficients and uncertainties in the atmospheric state (but not the instrumental noise since the S/N ratio is over 300:1). As a consequence (Fig. 4c), the effect of SD on the O_3 vmr vertical profile is significantly smaller than the statistical uncertainty (Fig. 4b) in this retrieved profile and would be even more negligible if systematic errors were included [23].

3.1.2. Limb-emission measurement

A similar (theoretical) exercise was made in the case of atmospheric emission spectra in the $10\ \mu\text{m}$ region, thus simulating space-borne experiments such as MIPAS [12]. It leads to the same conclusions as those obtained in the case of transmission spectra and to errors in the ozone vertical profile very similar to those in Fig. 1. Hence, again, the influence of SD on both the residuals and ozone vertical distribution remain much smaller than the uncertainties due to other sources (e.g., more than 5% in the O_3 vrm [24]).

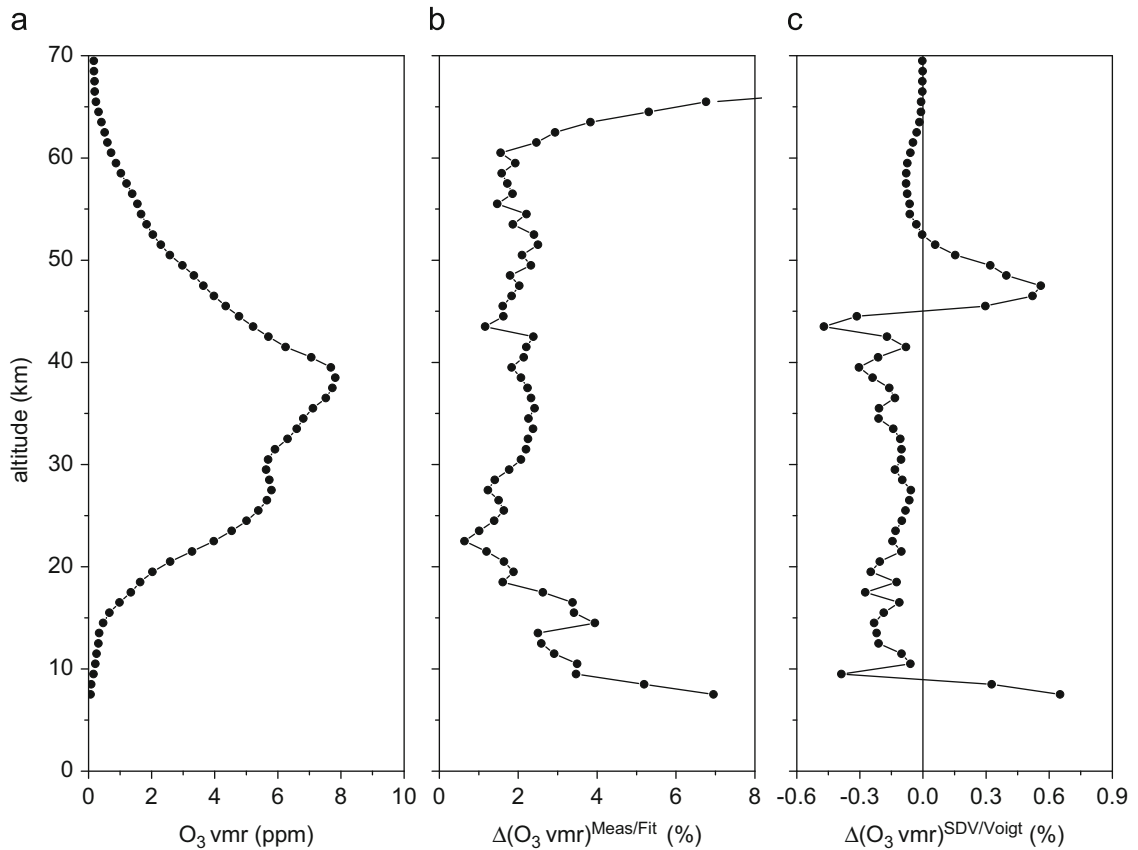


Fig. 4. Results of the treatment of ACE-FTS occultation ss28648. (a) Retrieved O₃ vertical profile. (b) Statistical uncertainty on the retrieved profile as obtained from the spectra fit residuals using speed dependent line shapes (nearly the same as the uncertainty obtained using Voigt profiles). (c) Difference between the O₃ amounts retrieved with speed dependent and pure Voigt line shapes.

3.2. Nadir and ground-based observations

3.2.1. Nadir emission

A high resolution radiance spectrum in the 10 μm region was computed using SDV line shapes and standard mid-latitude summer profiles to simulate nadir observations. It was then convolved using Gaussian (instrument) functions of various widths and the resulting radiances were inverted with a spectral model assuming pure Voigt line profiles. This retrieval was made with the radiative transfer model Karlsruhe Optimised and Precise Radiative transfer Algorithm (KOPRA) [25] and its numerical inversion module KOPRAFIT. This simulates what would be obtained in treatments of IASI [13], TES [26] or AIRS [14] data, for instance. The results are displayed in Figs. 5 and 6. As in the results of the previous section, Voigt line shapes may be used since this causes errors much smaller than those arising from other sources in both the fit residuals (Fig. 6) and the vertical profile (Fig. 5). Indeed, as shown in the right panel of Fig. 5 and in Refs. [27,28], the error estimates in the nadir ozone profile retrieved in the case of IASI are about 30% in the troposphere and have a minimum of around 5% in the stratosphere.

3.2.2. Ground-based transmission

The influence of SDV has also been examined by performing O₃ retrievals on a set of ground-based FTIR test spectra. These spectra have been recorded at the NDACC site at Kiruna (420 masl, 69°N) [29] and have been selected to cover the conditions encountered at this Arctic site (winter/summer, low/high airmass). The analysis of the test spectra has been performed with Version 9.6 of the retrieval code PROFFIT developed at IMK [30]. From Ver. 9.5 onwards, the code supports a speed-dependent-Galatry line-shape function (the SDV line shape being a special case of this generalized shape) [31]. Two retrieval runs have been performed for each spectrum, the SDV run and the reference run with the usual Voigt approach. For the retrieval of O₃, we applied a simplified version of the recipe suggested by Schneider and Hase [32]. As expected from the results of the previous sections, the observed influence of SDV on the retrieved O₃ profile, exemplified in Fig. 7, is minor. It is much smaller than systematic errors of current state-of-the-art ground-based FTIR instrumentation and analysis [33,34]. For instance, the systematic error bias due to line intensity and pressure broadening parameters are the leading contributions, and can be estimated to amount to about 2% and 1.6%,

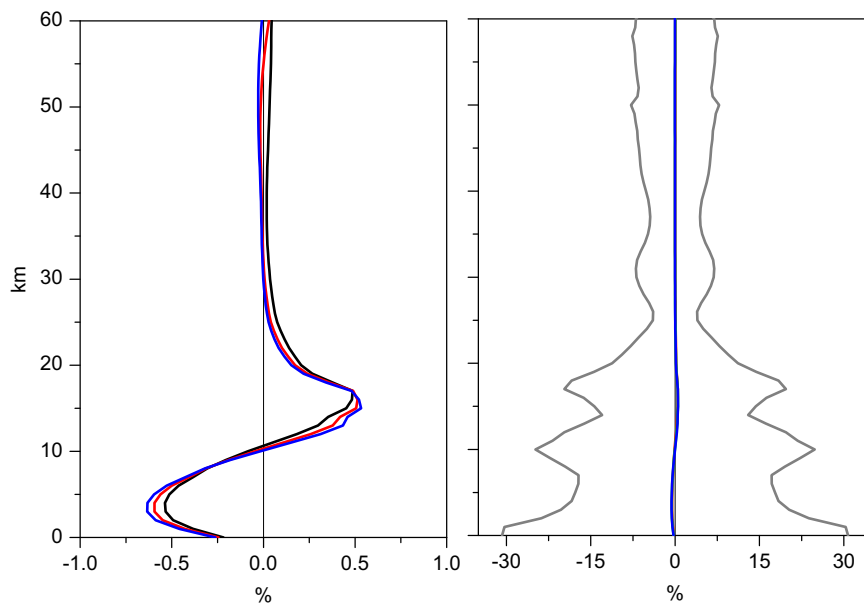


Fig. 5. Relative errors in the O_3 profiles obtained from fits of simulated nadir emission spectra caused by neglecting the speed dependence of the line broadening. The results are for Gaussian instrument functions of HWHM 0.20 (blue), 0.04 (red) and 0.008 (black) cm^{-1} . On the right panel, the grey curve represents the smoothing error. (For interpretation of the references to colour in this figure legend, the reader is referred to the web version of this article.)

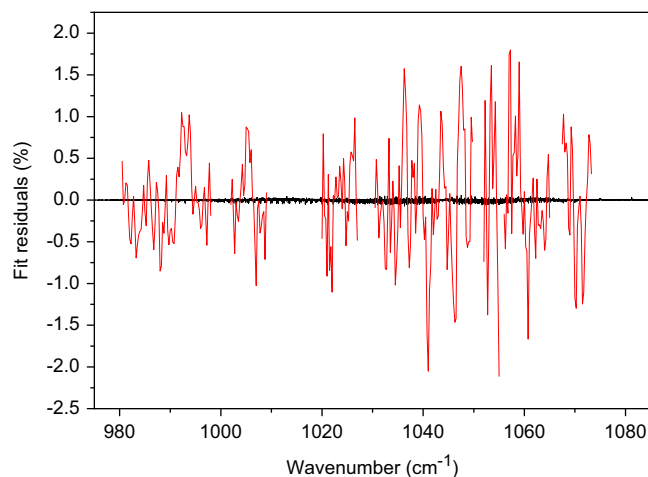


Fig. 6. Black curve is: residuals (in % of the “measured” radiance) in fits of simulated nadir spectra of O_3 with a resolution of 0.008 cm^{-1} caused by neglecting the speed-dependence (those for lower resolutions are even smaller). The red curve gives typical residuals obtained, in a selected set of micro-windows, from a fit of a measured IASI spectrum. (For interpretation of the references to colour in this figure legend, the reader is referred to the web version of this article.)

whereas the SDV correction changes the total column by about 0.1%. Furthermore, as in Fig. 3, the change in the fit residuals is completely negligible. These findings validating the Voigt profile are likely applicable to any NDACC-type measurement.

3.3. In situ laser measurements

Finally, “infinite” resolution absorption spectra of a single typical ozone line were computed for various

altitudes. This simulates observations such as those made using lasers on aircraft and below balloons (e.g., SDLA-LAMA [35], SPIRALE [15]). The (in situ) absorption calculated using the SDV line shape was adjusted using a Voigt profile, floating only the ozone local amount. The associated results (smaller errors and residuals would be obtained if the broadening coefficient was simultaneously adjusted, as done in the analysis of laboratory spectra) are plotted in Figs. 8 and 9. They show that, while fit residuals may be detected with high signal-to-noise measurements, the consequences on the ozone amount are lower than 1%.

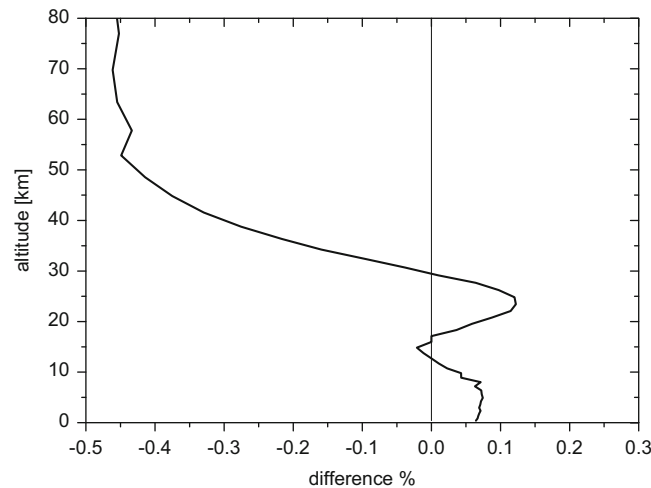


Fig. 7. Relative errors in the O_3 profile caused by neglecting the speed dependence of the line broadening obtained from the fit of a ground-based solar absorption spectrum recorded on 23 March 2003 at the NDACC site in Kiruna.

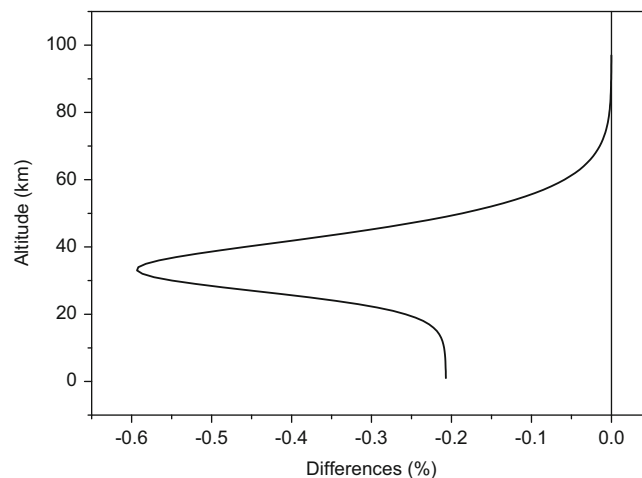


Fig. 8. Relative errors in the O_3 profile obtained from fits of in situ absorption coefficients caused by neglecting the speed dependence of the line broadening.

They thus again remain significantly smaller than the cumulative uncertainty due to other sources which total typically 4% [15]. These two findings are consistent with the results obtained for H_2O in Ref. [36]. Finally, note that the altitude dependence of the error in Fig. 8 results from the variation of SD effects with pressure. The SD effects are almost constant in the collisional regime (high pressure or low altitudes) where the Doppler effect can be neglected. They become negligible when the collisional broadening is much smaller than the Doppler width (low pressure or high altitudes) with a maximum under conditions (at about 10 hPa or 30 km for an O_3 line near 1000 cm^{-1}) where the Lorentz and Doppler width are comparable.

4. Conclusion

The present paper demonstrates that use of the Voigt profile for ozone for collisionally isolated lines in

atmospheric retrievals is a good approximation at this time. Indeed, the speed dependence (based on Ref. [8] this statement also applies to the contribution of Dicke narrowing) causes changes in both the fit residuals and the O_3 vertical distribution that remain significantly smaller than the uncertainties due to other sources including spectroscopy and the atmospheric state. Among these, the line intensities and broadening coefficients make a significant contribution which remains in the order of 2–3% [37]. These findings could be anticipated from the fact that it is essentially the integrated intensity (rather than the line shape) that provides the information and that the SDV and Voigt profiles, although spectrally different, have the same (unit) area. The conclusions of this paper may have to be reconsidered in the future for new well-characterized instruments, given a very precise knowledge of the P , T profiles, and once the uncertainties in the line intensities and widths have been reduced to below one percent. Finally, the influence of line-mixing,

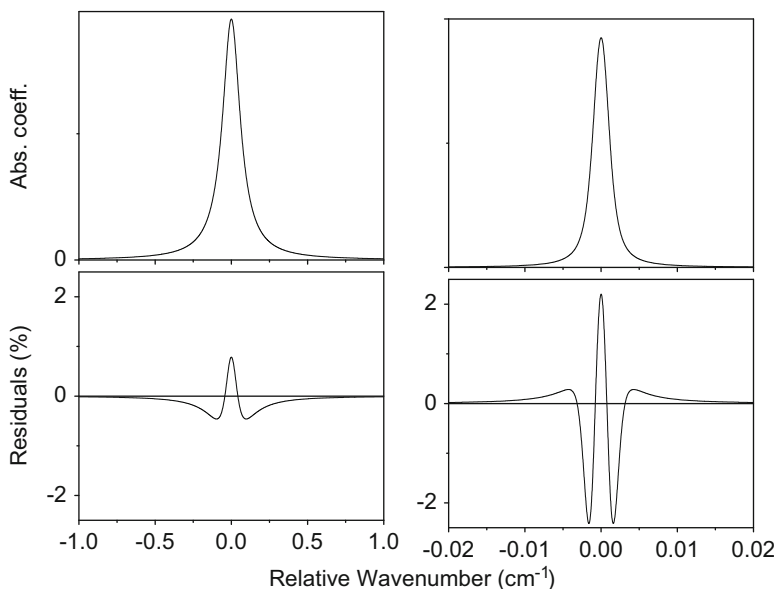


Fig. 9. Absorption line shapes of an O_3 line (top) and relative errors in their fits caused by neglecting the speed dependence for altitudes of 0 km (left) and 30 km (right). Note the difference in the wavenumber scale.

whose importance for retrievals of other species has been demonstrated (see Sec. VII.4 of Ref. [1] and the more recent results [38,39]), remains for ozone, an open issue. It is currently under study at LISA.

Acknowledgements

P. Bernath and C. Boone acknowledge support from the Canadian Space Agency and the UK Natural Environment Research Council (NERC) to the ACE mission. Authors from LISA thank the Institut für Meteorologie und Klimaforschung (IMK), Karlsruhe, Germany, for a license to use the KOPRA radiative transfer model. The Centre d'Etudes et Recherches Lasers et Applications, Lille, France, is supported by the Ministère chargé de la Recherche, the Région Nord-Pas de Calais, and the Fonds Européen de Développement Economique des Régions.

References

- [1] Hartmann JM, Boulet C, Robert D. Collisional effects on molecular spectra. Laboratory experiments and models, consequences for applications. Amsterdam: Elsevier; 2008.
- [2] Wang YJ. Effects of collisional narrowing and line parameters on atmospheric composition measurements. *JQRST* 1984;32:305–9.
- [3] Barret B, Hurtmans D, Carleer MR, De Mazière M, Mahieu E, Coheur PF. Line narrowing effect on the retrieval of HF and HCl vertical profiles from ground-based FTIR measurements. *JQRST* 2005;95:499–519.
- [4] Boone CD, Walker KA, Bernath PF. Speed-dependent Voigt profiles of water vapor in infrared remote sensing applications. *JQRST* 2007;105:525–32.
- [5] Mondelain D, Payan S, Deng W, Camy-Peyret C, Hurtmans D, Mantz AW. Measurement of the temperature dependence of line mixing and pressure broadening parameters between 296 and 90 K in the ν_3 band of $^{12}CH_4$ and their influence on atmospheric methane retrievals. *J Mol Spectrosc* 2007;244:130–7.
- [6] Schneider M, Hase F. Improving spectroscopic line parameters by means of atmospheric spectra: theory and example for water vapor and solar absorption spectra. *JQRST* 2009;110:1825–39.
- [7] Priem D, Colmont JM, Rohart F, Wlodarczak G, Gamache RR. Relaxation and lineshape of the 500.4-GHz line of ozone perturbed by N_2 and O_2 . *J Mol Spectrosc* 2000;204:204–15.
- [8] Rohart F, Wlodarczak G, Colmont JM, Cazzoli G, Dore L, Puzzarini C. Galatry versus speed-dependent Voigt profiles for millimeter lines of O_3 in collision with N_2 and O_2 . *J Mol Spectrosc* 2008;251:282–92.
- [9] D'Eu JF, Lemoine B, Rohart F. Infrared HCN lineshapes as a test of galatry and speed dependent Voigt profiles. *J Mol Spectrosc* 2002;212:96–110.
- [10] Rohart F, Nguyen L, Buldyreva J, Colmont JM, Wlodarczak G. Lineshapes of the 172 and 602 GHz rotational transitions of $HC^{15}N$. *J Mol Spectrosc* 2007;246:213–27.
- [11] Bernath PF, McElroy CT, Abrams MC, Boone CD, Butler M, Camy-Peyret C, et al. Atmospheric Chemistry Experiment (ACE): mission overview. *Geophys Res Lett* 2005;32:L15S01, doi:10.1029/2005GL022386.
- [12] Fischer H, Oelhaf H. Remote sensing of vertical profiles of atmospheric trace constituents with MIPAS limb-emission spectrometers. *Appl Opt* 1996;35:2787–96.
- [13] Clerbaux C, Hadji-Lazaro J, Turquety S, George M, Coheur PF, Hurtmans D, et al. The IASI/MetOp I mission: first observations and highlights of its potential contribution to GMES. *Space Res Today* 2007;168:19–24.
- [14] Aumann HH, Chahine MT, Gautier C, Goldberg MD, Kalnay E, McMillin LM, et al. AIRS/AMSU/HSB on the Aqua mission: design, science objectives, data products, and processing systems. *IEEE Trans Geosci Remote Sensing* 2003;41:253–64.
- [15] Moreay G, Robert C, Cataoie V, Chartier M, Camy-Peyret C, Huret N, et al. SPIRALE: a multispecies in situ balloon borne instrument with six tunable diode laser spectrometers. *Appl Opt* 2005;44:5972–5989.
- [16] Berman PR. Speed-dependent collisional width and shift parameters in spectral profiles. *JQRST* 1972;12:1331–42.
- [17] Ward J, Cooper J, Smith EW. Correlation effects in the theory of combined Doppler and pressure broadening—I. Classical theory. *JQRST* 1974;14:555–90.
- [18] Rothman LS, Gordon IE, Barbe A, Benner DC, Bernath PF, Birk M, et al. The HITRAN 2008 molecular spectroscopic database. *JQRST* 2009;110:533–72.
- [19] Abramowitz M, Stegun IA. In: Abramowitz M, Stegun IA, editors. *Handbook of Mathematical Functions*. NY: Dover Publications Inc.; 1972.
- [20] Rohart F, Mäder H, Nicolaisen HW. Speed dependence of rotational relaxation induced by foreign gas collisions: studies on CH_3F by millimeter coherent transients. *J Chem Phys* 1994;101:6475–86.
- [21] Air Force Geophysics Laboratory US Standard atmospheres from Optical properties of the atmosphere, 3rd ed., AFCRL-72-0497 (AD

- 753 075), US Standard atmosphere 1976 and Supplements 1966, plus collected constituent profiles.
- [22] Boone CD, Nassar R, Walker KA, Rochon Y, McLeod SD, Rinsland CP, et al. Retrievals for the atmospheric chemistry experiment Fourier-transform spectrometer. *Appl Opt* 2005;44:7218–31.
- [23] Dupuy E, Walker KA, Kar J, Boone CD, McElroy CT, Bernath PF, et al. Validation of ozone measurements from the Atmospheric Chemistry Experiment (ACE). *Atmos Chem Phys* 2009;9:287–343.
- [24] Gil-López S, López-Puertas M, Kaufmann M, Funke B, García-Comas M, Koukoulis ME, et al. Retrieval of stratospheric and mesospheric O₃ from high resolution MIPAS spectra at 15 and 10 μm. *Adv Space Res* 2005;36:943–51.
- [25] Stiller GP, editor, with contributions from von Clarmann T, Dudhia A, Ehle G, Funke B, Glatthor N, Hase F, Hopfner M, Kellmann S, Kemnitzer H, Kuntz M, Linden A, Linder M, Stiller GP, Zorn S. The Karlsruhe Optimized and Precise Radiative Transfer Algorithm (KOPRA). Vol. FZKA 6487 of Wissenschaftliche Berichte, Forschungszentrum Karlsruhe, Germany, 2000.
- [26] Beer R. TES on the aura mission: scientific objectives, measurements, and analysis overview. *IEEE Trans Geosci Remote Sensing* 2006;44:1102–5.
- [27] Keim C, Eremenko M, Orphal J, Dufour G, Flaud JM, Hopfner M, et al. Tropospheric ozone from IASI: comparison of different inversion algorithms and validation with ozone sondes in the northern middle latitudes. *Atmos Chem Phys* 2009;9:9329–47.
- [28] Ceccherini S, Cortesi U, Del Bianco S, Raspollini P, Carli B. IASI-METOP and MIPAS-ENVISAT data fusion. *Atmos Chem Phys Discuss* 2010;10:183–211.
- [29] Kopp G, Berg H, Blumenstock T, Fischer H, Hase F, Hochschild G, et al. Evolution of ozone and ozone related species over Kiruna during the THESEO 2000-SOLVE campaign retrieved from ground-based millimeter wave and infrared observations. *J Geophys Res D* 2003;108:8308.
- [30] Hase F, Hannigan JW, Coffey MT, Goldman A, Höpfner M, Jones NB, et al. Intercomparison of retrieval codes used for the analysis of high-resolution, ground-based FTIR measurements. *JQSRT* 2004;87:25–52.
- [31] Ciurylo R, Szudy J. Speed-dependent pressure broadening and shift in the soft collision approximation. *JQSRT* 1997;57:411–23.
- [32] Schneider M, Hase F. Technical note: recipe for monitoring of total ozone with a precision of around 1 DU applying mid-infrared solar absorption spectra. *Atmos Chem Phys* 2008;8:63–71.
- [33] Schneider M, Redondas A, Hase F, Guirado C, Blumenstock T, Cuevas E. Comparison of ground-based Brewer and FTIR total column O₃ monitoring techniques. *Atmos Chem Phys* 2008;8:5535–50.
- [34] Schneider M, Hase F, Blumenstock T, Redondas A, Cuevas E. Quality assessment of O₃ profiles measured by a state-of-the-art ground-based FTIR observing system. *Atmos Chem Phys* 2008;8:5579–88.
- [35] Durry G, Mégie G. Atmospheric CH₄ and H₂O monitoring with near-infrared InGaAs diodes by the SDLA, a balloon borne spectrometer for tropospheric and stratospheric in situ measurements. *Appl Opt* 1999;38:7342–54.
- [36] Durry G, Zéninari V, Parvitte B, Le Barbu T, Lefevre F, Ovarlez J, et al. Pressure broadening coefficients and line strengths of H₂O near 1.39 μm: application to the in situ sensing of the middle atmosphere with balloon-borne diode lasers. *JQSRT* 2005;94:387–402.
- [37] Guinet M, Mondelain D, Janssen C, Camy-Peyret C. Laser spectroscopic study of ozone in the 100–000 band for the SWIFT instrument. *JQSRT* 2010;111:961–72.
- [38] Hartmann JM, Tran H, Toon GC. Influence of line mixing on the retrievals of atmospheric CO₂ from spectra in the 1.6 and 2.1 μm regions. *Atmos Chem Phys* 2009;9:7303–12.
- [39] Tran H, Hartmann JM, Toon G, Brown LR, Frankenberg C, Warneke T, Spietz P, Hase F. The 2ν₃ band of CH₄ revisited with line mixing. Consequences for spectroscopy and atmospheric retrievals at 1.67 μm. *JQSRT*, in press.